Surface brightness profiles of dwarf galaxies in the NGC 5044 Group: A critical revision of the luminosity – shape relation as a distance indicator

Sergio A. Cellone

Facultad de Ciencias Astronómicas y Geofísicas, Universidad Nacional de La Plata, Paseo del Bosque, 1900 La Plata, Buenos Aires, Argentina
(scellone@fcaglp.unlp.edu.ar)

Abstract. CCD surface photometry of a small sample of dwarf and intermediate luminosity elliptical galaxies in the NGC 5044 Group is presented. Their surface brightness profiles are fitted with a Sérsic law, and it is shown that a few relatively bright galaxies with "convex" profiles destroy the known relation between total magnitude and the "shape" parameter (N) of the model, thus ruling out the use of this relation as a distance indicator for individual galaxies. Even eliminating these deviant galaxies, as well as those with poor quality profiles, the scatter of the luminosity – shape relation remains relatively high, despite that depth effects should not be important in this small group of galaxies. In addition, the fact that there is a lower limit in the size of galaxies which can be resolved in more distant clusters causes the observed luminosity – shape relation to change both its slope and its zero point as distance increases, limiting also its practical use as a distance indicator for groups of galaxies.

An alternative is explored using the known relation between integrated magnitude and effective surface brightness as a distance indicator, and it is found that its zero point also changes depending on the mean sizes of the galaxies included in each sample. Mean distances for groups of galaxies obtained with this method should then be taken with care.

The effects of seeing on the derived photometric parameters are also investigated in an empirical way.

Three very faint, previously non-catalogued, dwarf-spheroidal galaxies were also detected, and their photometric data are given, along with their coordinates.

Key words: galaxies: structure – galaxies: photometry – galaxies: fundamental parameters – galaxies: elliptical and lenticular, cD – galaxies: distances and redshifts – galaxies: clusters: individual: NGC 5044 Group

1. Introduction

The use of the luminosity profiles of dwarf elliptical (dE) galaxies as a distance indicator has been considered as a potentially powerful tool because of the large number of dEs in clusters of galaxies and the relative ease with which the profile parameters can be determined. Bothun et al. (1989) were the first to develop a method involving the surface brightness profiles of dEs, and applied it to the determination of the relative distances between the Virgo, Fornax, and Centaurus clusters. Basically, they fitted the profiles of their galaxies with exponential functions ($I_{(r)} = I_0 \, e^{-\frac{r}{\alpha}}$) and then selected, within each cluster, those galaxies with similar scale lengths (α); with these conditions, total magnitude depends only on central surface brightness (I_0), and the relative distributions of α can be used to derive the relative distance moduli to the clusters [Note that in the present paper α corresponds to α^{-1} using the notation of Bothun et al. (1989)]. This technique has the advantage of its simplicity, but the condition that galaxies with profiles departing from an exponential must be rejected restricts its use only to relatively rich clusters of galaxies.

The fact that useful information about the luminosity of dEs was present in the *shape* of their profiles was already known from several studies which had revealed that, although most dEs could be reasonably well fit by exponentials, brighter dEs tended to have a bulge-type component, while the fainter dwarfs usually had large, flat cores (Karachentseva et al. 1987; Caldwell & Bothun 1987; Impey et al. 1988). The first ones have then profiles more resembling an $r^{\frac{1}{4}}$ law, while the latter have profiles showing a curvature in the opposite way, i. e.: "concave" and "convex", respectively, in a surface brightness (in mag arcsec^{-2}) vs. r plot, where an exponential is a straight line. This luminosity – shape relation can be quantified using a Sérsic (1968) law, instead of an exponential, to fit the profiles. The Sérsic law

$$I_{(r)} = I_0 \, e^{-\left(\frac{r}{\alpha}\right)^N}, \tag{1}$$

in intensity units, or

$$S_{(r)} = S_0 + 1.086 \left(\frac{r}{\alpha}\right)^N \tag{2}$$

in mag arcsec^{-2} units (where S_0 is the central surface brightness), is a more flexible fitting formula because it includes a third free parameter (N) which controls the shape of the profile. Its popularity is now growing, as can be judged from a number of recent papers where it has been used to fit the profiles of dE galaxies [Davies et al. 1988; Young & Currie 1994, 1995; Cellone et

al. 1994 (hereafter CFG); Durrell et al. 1996; Durrell 1997], as well as bright E galaxies (Caon et al. 1993; Saglia et al. 1993a; D'Onofrio et al. 1994, 1997; Graham et al. 1996), and bulges of S galaxies (Andredakis et al. 1995; de Souza & dos Anjos 1998; Young et al. 1998). Note that both the de Vaucouleurs and the exponential laws are particular cases of the Sérsic law, with $N = 0.25$ and $N = 1$, respectively.

Caon et al. (1993) and D'Onofrio et al. (1994) have shown that the shape parameter N (n^{-1} with their notation) correlates with the global parameters of the Fundamental Plane for (bright) early-type galaxies, either the effective radius r_e or the absolute blue magnitude M_B. On the other hand, Young & Currie (1994) used the relation between M_B and N for a sample of dEs to derive a distance modulus $(m-M)_0 = 30.70 \pm 0.30$ for the Fornax Cluster. The same authors used an alternative relation between the scale length and N to estimate the individual distances to 64 Virgo Cluster dEs (Young & Currie 1995). However, it has been shown that this luminosity – shape ($L - N$) relation has a scatter too large to be useful for individual galaxies, and the resulting error in distance modulus can be larger than 2 magnitudes (Durrell et al. 1996; Durrell 1997). Later, Binggeli & Jerjen (1998) strongly criticized Young & Currie (1994, 1995) for the same reason, and clearly showed that using the $L - N$ relation for individual galaxies may lead to wrong results. (But see also Young & Currie 1998.)

Selection effects were explored by CFG, who showed that the $L-N$ relation for dwarf ellipticals can be spuriously caused when galaxies within a narrow range of isophotal surface brightness are selected for detailed surface photometry. In this way, relatively bright (faint) dwarfs with convex (concave) profiles could be excluded from the observed samples because of their higher (lower) than average surface brightnesses.

This paper presents new data for a small sample of dwarf members of the NGC 5044 Group of galaxies, with the idea of further investigating the $L - N$ relation in a relatively small group of galaxies where depth effects are minimized, placing emphasis on some observational problems which can affect it. Sect. 2 describes the observations, while the fitting of the surface brightness profiles is described in Sect. 3. In Sect. 4 the effects of seeing are investigated, and the practical use of the $L - N$ relation as a distance indicator is discussed in Sect. 5. The conclusions of this work are summarized in Sect. 6.

2. Sample selection and observations

The galaxies were taken from the catalogue of Ferguson & Sandage (1990, hereafter FS90), which lists 162 (true, likely, and possible) members of the NGC 5044 Group, 69% of which are classified as dwarfs, either elliptical or irregular. The authors give three different determinations of its distance modulus relative to the Virgo Cluster, ranging from $\Delta(m - M)_0 = 2.26$ to $\Delta(m - M)_0 = 1.5$ mag. Using their average value $\Delta(m - M)_0 = 1.85$ and a distance modulus for Virgo $(m - M)_V = 30.04$ (Ferrarese et al. 1996), a distance modulus $(m - M)_0 = 31.9$ is obtained for the NGC 5044 Group. The whole surveyed area is about 630 kpc across, and the core

radius of the group as given by FS90 is 12.6 arcmin, which corresponds to 88 kpc, or roughly $\frac{1}{3}$ the core radius of the Virgo Cluster ($r_c = 249$ kpc); hence, depth effects are expected to be lower in the NGC 5044 Group as compared to Virgo. Several regions within the projected area of the group were selected with the sole condition that at least two galaxies, classified as dwarfs, could fit within the useful field of the instrument (see below). This procedure maximized the efficiency in telescope time utilization, and, at the same time, it guaranteed that the objects were selected as "blindly" as possible, in order to avoid introducing further selection effects than those already present in the original catalogue, except for the unavoidable limit in magnitude. This limit was estimated at $B_T \simeq 18.5$ mag ($M_{B_T} \simeq -13.4$, with the adopted distance) for the instrumental setup to be used, but depending also on angular size and surface brightness. This is not a detection limit, but rather a limit set by the impossibility of measuring with accuracy the surface brightness profiles of the faintest dwarfs, which are usually small and very low surface brightness (LSB) objects (see below, and see also Sect. 4). The catalogue is said to include all galaxies with diameters at the $S_B = 27$ isophote larger than 16 arcsec; since a fraction of them have magnitudes up to $B_T = 19.8$ mag, an additional bias against the faintest galaxies was introduced in my sample.

Five such fields were observed with the 2.15 m telescope at CASLEO[1] (San Juan, Argentina) during two nights in May 1996, using a liquid-nitrogen-cooled direct camera equipped with a Tek 1024 CCD. The chip's gain and read-out noise were set to 1.98 electrons/adu and 9.6 electrons, respectively. A focal reducer provided a scale of 0.82 arcsec/pixel, resulting in a useful field ~ 9 arcmin in diameter. Both nights were photometric: May 10, when all V band images were obtained, and May 13, when the same fields were observed through a B filter. Each observation was fragmented into three or more shorter exposures, in order that cosmic-rays could be identified and excised from the individual images using a semi-interactive procedure before they were summed up. Table 1 gives the J1950 coordinates of the centre of each field along with the effective exposure times in B and V. The last column lists the dwarf galaxies included within each field, with the same numeration as in the catalogue (FS90), preceded by "N" (standing for "number").

Several standard stars fields (Landolt 1992) were also observed at different airmasses for deriving the transformation equations to the standard system. The IRAF package was used for de-biasing and flat-fielding purposes, as well as for most of the image processing and photometry. Dome flats were used to correct the V images, while twilight flats gave better results with the B frames. The final images were flat to $\sim 1\%$ of the sky level, with low spatial frequency variations up to $\sim 2\%$ in a few frames.

Three new dwarf galaxies were identified from visual inspection on two of the fields. They are named in this paper by

Table 1. Observations.

Field	α_c	δ_c	Exp. time (B) sec	Exp. time (V) sec	Galaxies
1	$13^h\,11^m\,07^s$	$-16°\,05'\,00''$	2700	3600	N29, N30
2	$13^h\,11^m\,39^s$	$-16°\,09'\,47''$	2280	1650	N34, N42, N49, *N49A*
3	$13^h\,11^m\,54^s$	$-16°\,16'\,00''$	2700	2400	N50, N51, N55, N66
4	$13^h\,12^m\,53^s$	$-16°\,20'\,19''$	1380	2100	N83, *N83A*, N95, *N95A*, N98, N99
5	$13^h\,13^m\,51^s$	$-15°\,45'\,44''$	2160	2700	N122, N124

Table 2. Coordinates of new galaxies.

Name	α_{1950}	δ_{1950}
N49A	$13^h\,11^m\,50.6^s$	$-16°\,08'\,38''$
N83A	$13^h\,12^m\,46.3^s$	$-16°\,18'\,11''$
N95A	$13^h\,12^m\,58.6^s$	$-16°\,22'\,37''$

Table 3. Global Parameters.

Name	Type	Memb.	M_V mag	$(B-V)_0$ mag
N29	d:E	1	-17.57 ± 0.01	0.84 ± 0.03
N30	dE,N	1	-17.23 ± 0.02	0.80 ± 0.03
N34	d:E,N	1	-16.43 ± 0.01	0.83 ± 0.03
N42	dE,N	1	-17.40 ± 0.01	0.75 ± 0.02
N49	Im III	1	-16.71 ± 0.01	0.49 ± 0.02
N49A	–	–	-12.07 ± 0.09	0.83 ± 0.22
N50	dEpec,N/BCDring	1	-17.31 ± 0.01	0.76 ± 0.02
N51	dE,N	1	-16.77 ± 0.03	0.91 ± 0.04
N55	dE	2	-12.66 ± 0.05	0.52 ± 0.10
N66	dE,N	1	-15.90 ± 0.02	0.75 ± 0.03
N83	dE	1	-15.86 ± 0.02	0.97 ± 0.04
N83A	–	–	-12.27 ± 0.04	0.85 ± 0.14
N95	dE,N?	1	-14.89 ± 0.02	0.93 ± 0.08
N95A	–	–	-14.15 ± 0.13	0.93 ± 0.31
N98	dE	3	-13.66 ± 0.09	1.11 ± 0.15
N99	? or dE	3	-12.12 ± 0.05	1.68 ± 0.25
N122	dE	1	-15.49 ± 0.02	0.67 ± 0.04
N124	dE(Displaced N),N?	2	-14.75 ± 0.04	0.94 ± 0.08

appending an "A" to the name of the nearest known dwarf (they are listed in italics in Table 1). Their coordinates, measured by offset from known objects in the same fields, are given in Table 2, with estimated accuracies of about 10 arcsec. Absolute V magnitudes and $(B-V)$ colours corrected for Galactic extinction ($E_{BV} = 0.03$, Burstein & Heiles 1984), along with morphological types and membership codes (1: definite, 2: likely, 3: possible) from FS90 are given in Table 3 for all observed galaxies. Two of the new galaxies (N49A, N83A) have luminosities comparable to those of Local Group dwarf spheroidals, while the third one (N95A) is nearly two magnitudes brighter than the faintest catalogued dEs in the group; it was probably not included in the catalogue because of its very low surface brightness.

Note that according to their absolute magnitudes the brightest galaxies in the present sample are not "true" dwarfs, but rather intermediate luminosity galaxies [or "low luminosity ellipticals", using the nomenclature given by Prugniel (1994)].

3. Surface brightness profiles

3.1. Elliptical isophotes fitting

As is usual when observing dwarf galaxies, there were plenty of sky pixels in all the frames; this is an advantage, because most dwarfs are LSB objects, and hence their profiles are strongly affected by small errors in the adopted sky level. A first sky subtraction was made on the individual images, fitting the sky level with a plane; after summing them up, the sky was checked again.

The program objects were then identified on the final images, and each galaxy was analyzed separately. Foreground stars as well as neighbour and background galaxies were masked out. The fitting of elliptical isophotes, along with the measurement of the surface brightness profiles, was made with the ELLIPSE task within STSDAS–IRAF, allowing the centre, ellipticity (ϵ), and position angle (φ) of each ellipse to vary freely, except for

the very inner and the outer regions, where they were fixed to the average values of the nearest 10–12 points. The inner region was defined as those isophotes with semi-major axis $a < 8$ pix ($6.5''$), where the small number of pixels of each isophote prevents a good convergence of the ellipse-fitting algorithm and seeing effects are stronger (see next section), while the outer region comprised those isophotes with a mean surface brightness fainter than the sky rms.

A final fine-tuning of the sky level (typically a few adu) was made by plotting the total flux vs. semi-major axis, and checking that the total flux attained a constant value for sufficiently large values of a (~ 2 arcmin, or roughly 17 kpc with the adopted distance). This method does not depend on any assumption about the shape of the profile, but it only requires that the luminous contribution from the galaxy vanishes far away from its centre (see for example Binggeli et al. 1984).

3.2. Model fitting

For each galaxy, the surface brightness profile (in magnitudes per square arcsecond) was plotted against the reduced radius ($r = a\sqrt{1-\epsilon}$), and a Sérsic function (Eq. 2) was fitted to the

Table 4. Parameters of the Sérsic law fits.

Name	S_0 mag arcsec^{-2}	α arcsec	N	ΔN	V_T mag	r_e arcsec	S_e mag arcsec^{-2}
N29	18.90 ± 0.02	0.95 ± 0.02	0.54 ± 0.00	-0.00	14.74 ± 0.07	9.4 ± 0.3	21.60 ± 0.03
N30	20.25 ± 0.02	2.77 ± 0.05	0.69 ± 0.00	-0.01	15.02 ± 0.05	10.6 ± 0.3	22.15 ± 0.03
N34	19.80 ± 0.02	1.09 ± 0.02	0.60 ± 0.00	-0.17	15.95 ± 0.06	6.8 ± 0.2	22.11 ± 0.03
N42	23.02 ± 0.02	17.43 ± 0.20	1.43 ± 0.02	-0.04	15.34 ± 0.04	18.4 ± 0.4	23.66 ± 0.03
N49	21.49 ± 0.01	7.10 ± 0.04	1.36 ± 0.01	-0.04	15.70 ± 0.02	7.9 ± 0.1	22.18 ± 0.01
N50	20.91 ± 0.01	6.93 ± 0.04	1.34 ± 0.01	-0.07	15.16 ± 0.02	7.8 ± 0.1	21.63 ± 0.01
N51	22.71 ± 0.10	8.35 ± 0.69	0.88 ± 0.04	-0.02	15.82 ± 0.25	17.9 ± 2.4	24.08 ± 0.14
N55	22.08 ± 0.15	0.78 ± 0.13	0.61 ± 0.03	-0.47	19.03 ± 0.50	4.6 ± 1.3	24.34 ± 0.23
N66	21.70 ± 0.03	3.63 ± 0.11	0.82 ± 0.01	-0.03	16.44 ± 0.09	8.9 ± 0.4	23.19 ± 0.05
N83	22.44 ± 0.02	6.10 ± 0.13	0.93 ± 0.02	0.02	16.37 ± 0.07	11.6 ± 0.5	23.69 ± 0.04
N95	20.40 ± 0.17	0.65 ± 0.12	0.55 ± 0.03	0.08	17.24 ± 0.54	5.6 ± 1.7	22.99 ± 0.25
N95A	16.00 ± 0.05	$< 1 \times 10^{-3}$	0.17 ± 0.00	0.16	17.09 ± 1.05	38.8 ± 28.3	27.03 ± 0.40
N98	13.78 ± 0.13	$< 1 \times 10^{-3}$	0.22 ± 0.01	$-$	18.07 ± 1.16	2.5 ± 2.1	22.04 ± 0.50
N122	21.18 ± 0.03	1.61 ± 0.05	0.64 ± 0.01	-0.03	16.77 ± 0.09	8.2 ± 0.4	23.32 ± 0.05
N124	15.15 ± 0.75	$< 1 \times 10^{-3}$	0.24 ± 0.02	0.16	17.08 ± 2.19	5.0 ± 15.9	22.56 ± 1.10

data, using the NFIT1D task within STSDAS–IRAF. The same inner and outer cutoffs in radius previously adopted for isophote fitting (see Sect. 3.1 above) were set for the profile fitting algorithm. This ensured that those data points more heavily affected by seeing (see Sect. 4) and by sky noise were not included in the fit. Prominent nuclei or small bulge components were excluded from the fits (in N42 and N51) as well as "bumps" in the outer regions of two profiles, caused by an extended LSB feature in N122, and probably by a foreground or background object not properly masked out in N34.

The three parameters of the model (S_0, α, and N), along with their respective errors, are given in Table 4. The errors were estimated in the following way: the sky brightness was varied in plus/minus its mean error (normally a few adu), and then the profile was re-computed and a new fit was made. This procedure gave larger (and probably more realistic) error estimates than the formal errors provided by the NFIT1D task, so the former were adopted. An additional check of the stability of the fits was made by re-fitting the profiles after changing the outer radial cutoff to the isophote with $I_{(r)} = \frac{1}{2}\sigma_{\rm SKY}$. The difference ($\Delta N$) between the value of N obtained with this last ($\frac{1}{2}\sigma$) cutoff and the original (1σ) one was calculated and is also shown in Table 4.

Some of the resulting surface brightness profiles, along with V band images of the corresponding galaxies, are shown in Fig. 1. (All the images are displayed using the same range of grey-scale levels.) While fits to bright (and large) galaxies give very stable results, the results for the fainter (and also smaller) dwarfs are affected both by a lower signal-to-noise ratio and by the fact that the range between the inner and outer radial cutoffs is very small. For three galaxies (N49A, N83A, N99) no fit was at all possible since their profiles did not extend much further than the seeing PSF. Four other galaxies (N55, N95A, N98, and N124) produced very unstable fits, as can be judged from their large ΔN values. I will return to them in Sect. 4, while discussing seeing effects.
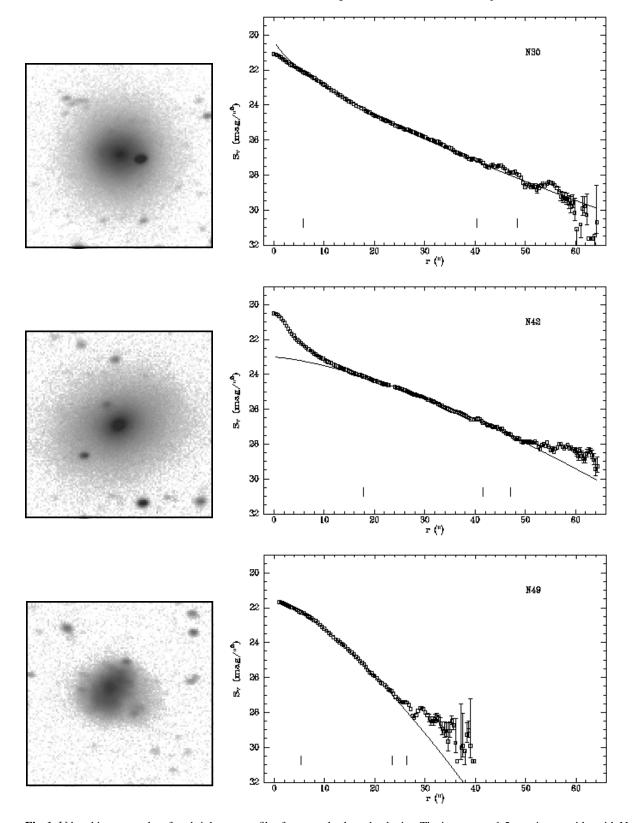
Fig. 1 illustrates the fact that the Sérsic law fits fairly well most of the profiles, except for their innermost and outermost regions, turning the choice of the range in radius over which the fit will be done into a crucial point (Durrell 1997). Nearly exponential or convex-shaped models ($N \gtrsim 1$) usually fall below the brightness enhancements due to nuclei or central bulge-type components (e. g.: N42, N50, N51), while concave-shaped models ($N < 1$) tend to overestimate the central surface brightnesses when no prominent nucleus is present (e. g.: N30). Although this last behaviour is enhanced with bad seeing, it is usually observed under fairly good seeing conditions (CFG; Durrell 1997). An extreme example is given by N95A, where the strong coupling between the three parameters of the Sérsic law produces a spuriously high central surface brightness. Regarding N42, attempts to fit two different Sérsic laws, one for the inner bulge-type component and another one for the main body of the galaxy, give varying results depending on the limits in radius selected for each fit. In any case, most solutions give large N values ($N > 1.5$) for the outer, main component of the galaxy. On the other hand, the outer portion of the profile of N50 shows what seems to be the effect of a bright star ($V \simeq 16$) some 30 arcsec from the centre of the galaxy. This up-turning portion of the profile lies beyond the 1σ cutoff (and below $S_V = 27$ mag arcsec^{-2}), and is thus not considered as a real feature of the galaxy.

Total V magnitudes were calculated integrating Sérsic's law (Eq. 1) to infinity, giving:

$$V_T = S_0 - 2.5 \log(2\pi\alpha^2) - 2.5 \log\left[\frac{\Gamma\left(\frac{2}{N}\right)}{N}\right]. \tag{3}$$

The effective radius (or half–light radius, r_e) has no analytical expression, so it was obtained numerically for each galaxy. The mean surface brightness within the effective radius (S_e) was then calculated as

$$S_e = V_T + 5 \log(r_e) + 2.5 \log(2\pi), \tag{4}$$

Fig. 1. *V* band images and surface brightness profiles for several selected galaxies. The images are 1.5 arcmin on a side, with North up and East to the left. Small ticks below the profiles show the inner (8 pix) and the two outer (1σ and $\frac{1}{2}\sigma$) cutoffs in radius for model fitting. The fitted models are shown with solid lines. Error bars are not shown when they are smaller than the symbol size.
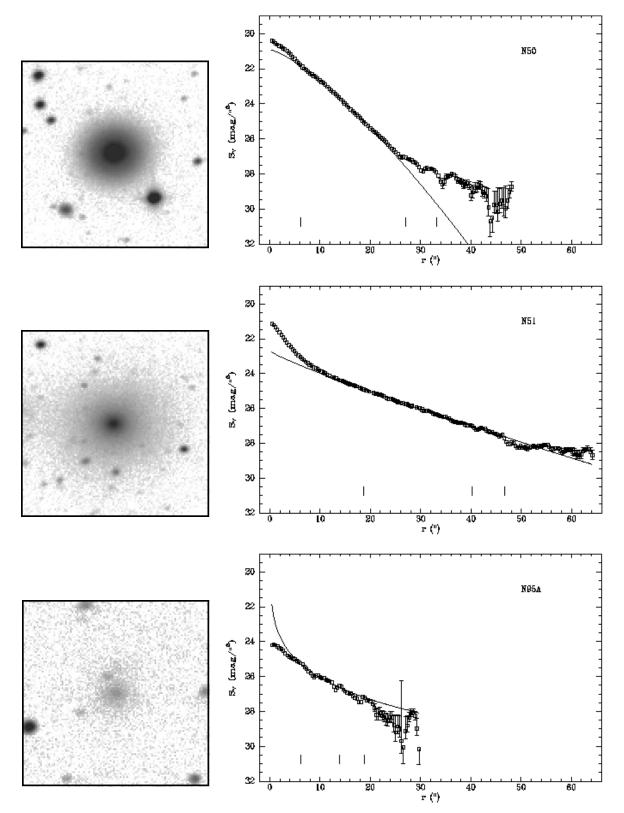
Fig. 1. (Continued)

or

$$S_{\rm e} = S_0 + 5 \log\left(\frac{r_{\rm e}}{\alpha}\right) - 2.5 \log\left[\frac{\Gamma(\frac{2}{N})}{N}\right]. \qquad (5)$$

It can be shown that $\frac{r_{\rm e}}{\alpha}$ depends only on N, and then $S_{\rm e}$ does not depend on α. These calculated parameters are also shown in Table 4. The magnitudes and colours in Table 3, instead, were obtained from the observed profiles with no model assumption, to allow for those galaxies whose profiles couldn't be fitted with the model.

4. Seeing effects

The effects of seeing on the photometric parameters of elliptical galaxies have been studied using different techniques (e. g.: Franx et al. 1989; Peletier et al. 1990; Saglia et al. 1993b). These studies have shown that the effects of seeing on surface brightness and ellipticity profiles may extend up to several PSF radii.

The observations presented in this paper were obtained under rather mediocre seeing conditions and, in addition, the telescope had small tracking errors. This resulted in a non-circular PSF, with Gaussian fits to its minor and major axis giving $\mathrm{FWHM}_Y \simeq 2.0''$ and $\mathrm{FWHM}_X \simeq 2.8''$, respectively, with small variations between different frames. However, the actual shape of the PSF was not Gaussian, having notably larger wings. The adopted approach, then, was to evaluate the effects of seeing on this particular set of observations using an empirical PSF obtained from the same data using IRAF–DAOPHOT routines. A set of artificial galaxies following a perfect Sérsic law and spanning a broad range in the relevant parameters was generated, and then convolved with the empirical PSF. The surface brightness profiles of these convolved artificial galaxies were then obtained and fitted with a Sérsic law, in the same way as was previously done with the observed galaxies. The effects of seeing were evaluated by comparing the "observed" and the "original" parameters for the convolved artificial galaxies.

A total of 55 artificial galaxies were generated with fixed central surface brightness, and spanning the following ranges in scale length and shape parameter: $0.001'' \le \alpha \le 10''$, and $0.25 \le N \le 1.50$, respectively. Most of them were round, but several non-circular ($\epsilon = 0.5$) and a few "nucleated" artificial galaxies (i. e., with a point source 10% the luminosity of the galaxy added at its centre, before the convolution) were also generated, in order to check for any differences compared to circular, non-nucleated galaxies. No noise or constant sky level were added. Although a complete study of seeing and instrumental effects would require the inclusion of these factors, along with the generation of a larger sample of artificial galaxies convolved with different PSFs, the present approach is sufficient to evaluate the global effects of seeing on the measured photometric parameters of this particular sample of galaxies.

Fig. 2 shows the differences between each measured parameter and the original one [ΔS_0, $\Delta \log(\alpha)$, and $\Delta \log(N)$, respectively] against the measured effective radius $r_{\rm e}$. It is evident that for sufficiently large galaxies the original parameters are recov-
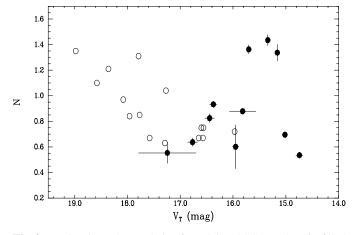

Fig. 2a–c. Measured (after convolution with PSF) minus original parameters against measured effective radius for 55 artificial galaxies: **a** central surface brightness, **b** logarithm of scale length, and **c** logarithm of shape parameter. Squares: round, non-nucleated galaxies; triangles: $\epsilon = 0.5$, non-nucleated galaxies; crosses: round, nucleated galaxies. Dashed lines are least-squares fits for $\log(r_{\rm e}) \le 0.5''$.

ered with small errors, but for galaxies with $r_{\rm e} \lesssim 5''$ the parameters are systematically underestimated because of seeing and sampling effects. (Note that, at least in principle, it seems possible to recover the original parameters for the smaller galaxies; however, the scatter is large, specially for N, and trying to apply

Fig. 3. Luminosity – shape relation for NGC 5044 Group dwarfs (filled circles) and Fornax Cluster dwarfs form CFG (open circles).

a correction to individual objects may lead to meaningless results.) The few nucleated and flattened artificial galaxies follow the same trend as round, non-nucleated ones.

Four galaxies in the present sample have N values too low for their luminosity. They were already mentioned in the preceding section because of the poor quality of their profile fits. Three of them (N55, N98, and N124) have $r_e \leq 5''$, and so it is assumed that their observed parameters are flawed by seeing. [Alternatively, N98 may be a background object, as judged from its red colour (see Table 3); the same holds true for N99 (see Sect. 3.2).] The fourth one (N95A) has a formally large measured effective radius; however, its associated error, as well as ΔN, are abnormally large (the quality of its fit is very poor), and so its measured parameters are most probably wrong. Hence, these four galaxies will not be included in the following analysis. N95 has $r_e = 5.6''$, i.e., very near to the boundary where seeing effects begin to be significant; it is retained within the sample, although with caution since its N is then probably underestimated.

5. The luminosity – shape relation

The $L - N$ relation for the remaining 11 dwarfs in the NGC 5044 Group sample is plotted in Fig. 3 (filled circles). Also shown are 15 Fornax Cluster dwarfs from CFG (open circles). The V magnitudes for the Fornax dwarfs were calculated from their T_1 magnitudes using the transformations of Geisler (1996), and assuming a difference in distance moduli between NGC 5044 and Fornax $\Delta(M-m)_{\mathrm{N5044-F}} = 1.60$ mag (FS90), and a difference in reddenings $\Delta E_{BV_{\mathrm{N5044-F}}} = 0.03$ (Burstein & Heiles 1984).

It is clear that most of the NGC 5044 dwarfs merge with and extend towards brighter magnitudes the $L - N$ relation for Fornax dwarfs, making evident that the former belong to a population of intrinsically brighter objects than the Fornax sample. However, three galaxies (N42, N49, and N50) clearly depart from the relation, with shape parameters N too high (i. e., too "convex" profiles) for their luminosities. These are bright, relatively large dwarfs, with high signal-to-noise profiles, and

so their observed parameters are reliable. It is necessary then to explore whether any peculiarity is the cause of the abnormally large N values for these three galaxies.

5.1. The three "outliers"

It has been argued that galaxies with different stellar populations from most galaxies in a given sample are likely to have different structural parameters, departing then from the $L - N$ relation (Young & Currie 1998). N49 clearly stands out of my sample with a very blue colour $B - V = 0.49$; it is classified as Im III, which is evident from Fig. 1, where several blobs can be seen on an irregular LSB body. Its profile was fitted with a Sérsic law with $N = 1.36$; however, two exponentials with different slopes could have also worked well.

N50, in turn, is classified as *peculiar* or *ringed blue compact dwarf*; however, no peculiar morphology is evident from my images, which show very symmetric isophotes. (It can be argued that seeing may have smoothed out any subtle feature; however, note that the irregular morphology of N49 is clearly evident, despite of seeing.) Moreover, its colour is only 1 sigma lower than the mean for the whole sample ($\langle B - V \rangle = 0.84 \pm 0.16$), and far too red for a BCD (e. g.: Thuan 1983). The new photometry presented here shows that N50 may indeed be termed "compact", although surely not "blue". Its compact appearance is then not due to current star formation or a significantly younger population dominating its overall luminosity.

Finally, N42 is classified as a normal nucleated dwarf elliptical; its profile shows a very bright nucleus and a bulge-type component extending out to $\approx 18''$, but the outer, main portion of the profile is clearly convex, yielding $N = 1.43$. Its colour is similar to that of N50, i. e., not significantly lower than the mean of the sample. Note that with the usual practice (at least for bright ellipticals) of plotting surface brightness against $r^{\frac{1}{4}}$, which puts too much emphasis on the inner portions of the profile, N42 seems to be well fit by a de Vaucouleurs law, except for its outer regions, as if it were tidally truncated. However, the nearest massive galaxy, the SB0 NGC 5030 ($M_B = -17.7$), lies at a projected distance of 6.1 arcmin (~ 43 kpc). Instead, the projected distance from the SBa NGC 5035 ($M_B = -18.0$) to N50 is only 3.6 arcmin (~ 25 kpc), so there is a higher probability for this dwarf than for N42 to be tidally affected by a massive neighbour, although no conclusive evidence is available in either case.

So, only N49 should be excluded from the sample because of its stellar content being different from normal dEs. N42 and N50 are then genuine dwarf or intermediate – luminosity ellipticals that do not obey the $L - N$ relation. Note that their V_T are at least 3 mag brighter than predicted by their N values. The alternative of their being foreground objects is ruled out by the results of low resolution spectroscopy obtained with the same telescope on April 1997. A preliminary reduction of these data gave $v_r = 2660 \pm 180 \, \mathrm{km \, s^{-1}}$ for N42, and $v_r = 2390 \pm 130 \, \mathrm{km \, s^{-1}}$ for N50, i. e., both in very good agreement with the radial velocity of NGC 5044 itself as well as the only two other bright early type galaxies with known redshifts in the group

(Huchra et al. 1983). Unfortunately, no spectroscopic data are available for N49. The radial velocities of N42 and N50 thus confirm their classification as definite members of the group by FS90 on a morphological basis. It is important to test this morphological criterion, since it has been successfully verified in nearby clusters (Binggeli et al. 1993), but it fails for more distant clusters, like Coma (e. g.: Adami et al. 1998). A detailed spectroscopic study of a few galaxies from this sample will be presented in a forthcoming paper (Cellone, in preparation).

5.2. The role of surface brightness

The data presented in this paper support the claim that the $L-N$ relation is inappropriate as a distance indicator for individual galaxies. However, it could still be useful for a group of galaxies from which very deviant objects could be eliminated. To explore this I compared the NGC 5044 dwarfs with the large (photographic) Virgo Cluster sample of Binggeli & Jerjen (1998). Total blue magnitudes (B_T) for the NGC 5044 dwarfs were calculated from V_T and $(B-V)_0$, and the N values from the V band fits were used, instead of fitting the (generally noisier) B profiles. This assumes that there are no meaningful colour gradients, which is normally true for dEs (Caldwell & Bothun 1987; CFG; Durrell et al. 1996; Durrell 1997).

Fig. 4 shows $\log(N)$ against B_T for Virgo (all triangles) and NGC 5044 Group dwarfs (filled circles). The large scatter for the Virgo sample data, on which Binggeli & Jerjen (1998) based most of their strong critique to the use of the $L-N$ relation for distance determination purposes, is evident. With the inclusion of the "three outliers" and the probably undersampled N95 the scatter of the NGC 5044 Group data is even worse; although it is substantially reduced when these four galaxies are eliminated. The dashed line is a least-squares fit to the whole Virgo sample (rms = 0.9), while the solid line is a fit using the same slope to the seven remaining dwarfs in the NGC 5044 Group (rms = 0.7). (Note that the scatter is still relatively large, despite all troublesome galaxies were eliminated and just a handful of dwarfs with well determined profiles remained.) However, these two fits cannot be used as they are to derive a relative distance, because both samples are not directly comparable. It was shown in Sect. 4 that the profile parameters of galaxies with smaller angular sizes cannot be accurately measured; hence, the more distant sample will have a distribution of intrinsic sizes biased against small galaxies.

It is known that structural parameters of dEs are all connected to each other leading to a variety of different relations between them. In particular, any measure of the size (scale parameter α, effective or isophotal radii, etc.) correlates with luminosity (e. g.: Impey et al. 1988), and hence, smaller galaxies are in general fainter. This leads to a change in both zero point and slope for the $L-N$ relation when the intrinsically smaller galaxies are eliminated, as can be seen in Fig. 4, where the dotted line is a fit to a subsample of the Virgo data (half-filled triangles) formed after eliminating those galaxies that would have $r_e < 6.8''$ at the distance of NGC 5044. A relative distance modulus $\Delta(m-M) = 1.85$ was assumed (see Sect. 2), and the

Fig. 4. Logarithm of shape parameter (N) vs. apparent blue magnitudes for NGC 5044 Group dwarfs (filled circles), and Virgo dwarfs from Binggeli & Jerjen (1998) (all triangles). The Virgo subsample formed by those gala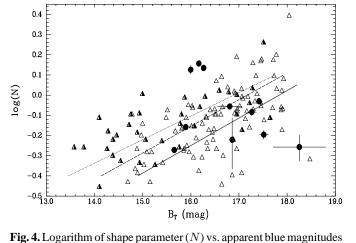xies which would have $r_e < 6.8''$ if their distance is incr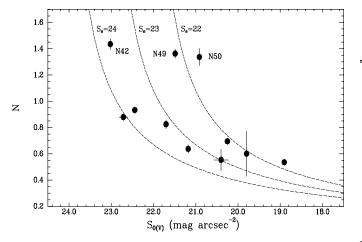eased by $\Delta(m-M) = 1.85$ are shown as half-filled triangles. The solid line is a linear fit to the NGC 5044 Group data, while the dashed and dotted lines are fits to the whole Virgo sample and subsample, respectively.

cutoff at $r_e < 6.8''$ was adopted because this is the lower limit for the NGC 5044 sample once N95 is also eliminated.

This Virgo subsample and the NGC 5044 data were then compared to obtain a new relative distance modulus, which in turn was used to define a new subsample, and this iterative procedure was repeated until it converged. A relative distance modulus $\Delta(m-M)_0 = 0.9 \pm 0.2$ was obtained, significantly lower than all previous determinations. This result should be taken with extreme caution, given the various explicit and implicit assumptions that were made. In particular, the goal of the procedure just described is that both samples span the same range in intrinsic effective radii; however, even if this goal is achieved, there is no guarantee that both samples have the same distribution of intrinsic effective radii. On the other hand, note that my sample lacks any faint galaxies with $N > 1$; this fact is probably introducing an additional bias in the $L-N$ relation for the NGC 5044 Group. A larger sample observed under better seeing conditions is clearly needed.

Regarding the large scatter of the $L-N$ relation, it was suggested that it could be reduced by adding a third parameter, probably surface brightness (Young & Currie 1994; Ferguson & Binggeli 1994). The role of surface brightness was also noted by CFG, who showed that their sample of Fornax dEs was bounded by curves of constant isophotal surface brightness in a central surface brightness vs. shape parameter plot. They suggested the existence of bright, relatively high surface brightness dwarfs with $N > 1$ (as well as faint, very LSB dwarfs with $N < 1$) that were not included when selecting a particular sample because their isophotal surface brightnesses were higher (lower) than the average. A similar plot is show in Fig. 5, where curves of constant effective surface brightness are drawn. Again, N42, N49, and N50 detach from the rest; in particular, N50 is located where CFG predicted bright galaxies with convex
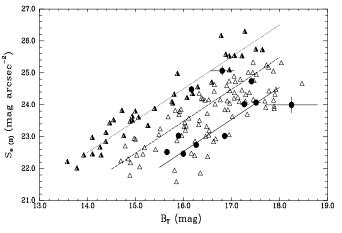
Fig. 5. Shape parameter vs. central surface brightness for NGC 5044 Group dwarfs. The dashed lines correspond to objects with constant effective surface brightnesses: $S_e = 22$, $S_e = 23$, and $S_e = 24$ mag arcsec^{-2}, as labeled. The three "outliers" are indicated.

Fig. 6. Effective surface brightness (S_e) vs. apparent blue magnitudes for NGC 5044 Group and Virgo dwarfs. Coding is the same as for Fig. 4

profiles could be found. However, N42 has a normal effective surface brightness (for LSB dwarfs), still its shape is abnormal for its luminosity.

Binggeli & Jerjen (1998) used a linear combination of central surface brightness (S_0) and $\log(N)$ to improve the correlation against total magnitude. However, they pointed out that nearly the same results were obtained using the relation between effective surface brightness (S_e) and total magnitude. In fact, S_e is a function of S_0 and N only (see Eq. 5), and has the advantage of being a "natural" combination of these parameters, then not depending on sample definition. Moreover, this relation is independent of Galactic extinction.

Fig. 6 is a plot of $S_{e(B)}$ against B_T for Virgo and NGC 5044 dwarfs, with the same codings as Fig. 4. The dashed line is a linear fit to the whole Virgo sample, and the dotted line is a fit to the subsample (half-filled triangles) formed with those Virgo galaxies that would have $r_e \geq 6.8''$ at the distance of NGC 5044. Both fits have fixed slope = 1.0, because this is by definition the slope of the S_e vs. V_T relation when $r_e = $ constant (see Eq. 4). Here, the effect of distance on the distribution of observed effective radii is even more dramatic than in Fig. 4.

The solid line is a fit to the NGC 5044 Group data (filled circles), excluding N42 and N51 (see below). It is evident that after the smaller dwarfs (affected by seeing) were eliminated, most of the remaining galaxies have similar effective radii (see Table 4) then producing a good correlation between S_e and B_T, except for N42 and N51 which are larger and then lie up and to the left of the mean relation. Again, a distance modulus between Virgo and the NGC 5044 Group can be derived, and then used to redefine the subsample, etc. This iterative procedure converged to $\Delta(m - M) = 2.20 \pm 0.08$, in good agreement with the value $\Delta(m - M) = 2.26$ obtained by FS90 using the brightest cluster member method. With this relative distance, N42 and N51 would be larger than the largest dwarf in the Virgo sample, then their exclusion is justified. This use of the effective surface

brightness vs. luminosity relation as a distance indicator is then equivalent to matching the mean effective radii of both samples.

It is illustrative to note that, when comparing the NGC 5044 Group data with the CCD photometry of a sample of Virgo dwarfs from Durrell (1997) or the Fornax data from CFG, the iterative procedure just described fails because the nearby samples almost vanish after the first iteration. For this method to work, then, the more distant cluster must be observed with the sufficient spatial resolution in order that objects with the same intrinsic sizes are included in both samples.

6. Conclusions

It is clear that the shape – luminosity relation cannot be used to derive distances to individual objects, at least until the situation of bright dwarfs with convex profiles, like N42 and N50, is understood. On the other hand, its use to derive mean relative distances for groups of galaxies is severely hampered by the fact that its slope changes when objects of different intrinsic effective radii are compared. This requires that samples with the same distribution of intrinsic sizes must be observed, a goal that is usually not easy to achieve. The data presented in this paper for several NGC 5044 Group dwarf and intermediate luminosity ellipticals were compared to a specially selected sample of Virgo dwarfs, trying to fulfill that condition. However, the relative distance obtained in this manner was significantly lower than all published values, suggesting that a systematic difference (maybe observational and/or environmental) is still present between both groups of dwarfs. It is also worth mentioning that, despite all galaxies with poor quality fits to their profiles, along with evident outliers, were eliminated, remaining then only dwarfs with good quality CCD profiles, the scatter of the $L - N$ relation remains relatively high, and this cannot be assigned to a depth effect, given the small size of the NGC 5044 Group as compared to the Virgo Cluster.

A relative distance between the two groups in good agreement with published values is obtained with the known luminosity vs. effective surface brightness relation. However, given the

small size of the NGC 5044 Group sample, and the unknown reliability of the procedure used for equalizing both samples, this result should be taken with care. Perhaps the $L - N$ relation, including its exceptions, is then more useful for studying the structure of elliptical galaxies than as a precise distance indicator. With this idea, it would be interesting to explore any possible connection between the shape parameter and other properties of the galaxies, such as velocity dispersion or metallicity. Environmental effects should also be investigated; it is interesting that two bright dwarfs with convex profiles were found in a blindly selected, although small sample of the NGC 5044 Group, while no counterparts are known in Virgo and Fornax. CCD surface brightness profiles for larger samples of dwarfs and intermediate luminosity ellipticals, including other nearby small groups, are needed to establish the statistical significance of this kind of galaxies.

References

Adami C., Nichol R.C., Mazure A., et al., 1998, A&A 334, 765

Andredakis Y.C., Peletier R.F., Balcells M., 1995, MNRAS 275, 874

Binggeli B., Jerjen H., 1998, A&A 333, 17

Binggeli B., Popescu C.C., Tammann G.A., 1993, A&AS 98, 275

Binggeli B., Sandage A., Tarenghi M., 1984, AJ 89, 64

Bothun G.D., Caldwell N., Schombert J.M., 1989, AJ 98, 1542

Burstein D., Heiles C., 1984, ApJS 54, 33

Caldwell N., Bothun G.D., 1987, AJ 94, 1126

Caon N., Capaccioli M., D'Onofrio M., 1993, MNRAS 265, 1013

Cellone S.A., Forte J.C., Geisler D., 1994, ApJS 93, 397 (CFG)

Davies J.I., Phillipps S., Cawson M.G.M., Disney M.J., Kibblewhite E.J., 1988, MNRAS 232, 239

de Souza R.E., dos Anjos S., 1998, In: Barbuy B., Lapasset E., Baptista R., Cid Fernandes R. (eds.) Proceedings of Workshop: Science with Gemini, (IAG–USP & UFSC), p. 128

D'Onofrio M., Capaccioli M., Caon N., 1994, MNRAS 271, 523

D'Onofrio M., Capaccioli M., Zaggia S.R., Caon N., 1997, MNRAS 289, 847

Durrell P.R., 1997, AJ 113, 531

Durrell P.R., McLaughlin D.E., Harris W.E., Hanes D.A., 1996, ApJ 463, 543

Ferguson H.C., Binggeli B., 1994, A&AR 6, 67

Ferguson H.C., Sandage A., 1990, AJ 100, 1 (FS90)

Ferrarese L., Freedman W.L., Hill R.J., et al., 1996, ApJ 464, 568

Franx M., Illingworth G., Heckman T., 1989, AJ 98, 538

Geisler D., 1996, AJ 111, 480

Graham A., Lauer T.R., Colless M., Postman M., 1996, ApJ 465, 534

Huchra J., Davis M., Latham D., Tonry J., 1983, ApJS 52, 89

Impey C.D., Bothun G.D., Malin D.F., 1988, ApJ 330, 634

Karachentseva V.E., Karachentsev I.D., Richter G.M., von Berlepsch R., Fritze K., 1987, Astron. Nachr.308, 247

Landolt A.U., 1992, AJ 104, 340

Peletier R.F., Davies R.L., Illingworth G.D., Davis L.E., Cawson M., 1990, AJ 100, 1091

Prugniel P., 1994, In: Meylan G., Prugniel P. (eds.) ESO/OHP Workshop Dwarf Galaxies, ESO, Garching, p. 171

Saglia R.P., Bender R., Dressler A., 1993a, A&A 279, 75

Saglia R.P., Bertschinger E., Baggley G., et al., 1993b, MNRAS 264, 961

Sérsic J.L., 1968, Atlas de Galaxias Australes. Observatorio Astronómico de Córdoba

Thuan T.X., 1983, ApJ 268, 667

Young C.K., Currie M.J., 1994, MNRAS 268, L11

Young C.K., Currie M.J., 1995, MNRAS 273, 1141

Young C.K., Currie M.J., 1998, A&A 333, 795

Young C.K., Metcalfe N., Zhu J., Wu H., Chen J., 1998, A&AS 130, 173